Acta Cryst. (1988). A**44**, 433-436

Observation of *Pendellösung* Fringes Induced by X-ray Resonant Scattering

By M. Yoshizawa, T. Fukamachi and K. Ehara

Saitama Institute of Technology, Ohsato, Saitama 369-02, *Japan*

T. Kawamura

Department of Physics, Yamanashi University, Kofu, Yamanashi 400, *Japan*

and K. Hayakawa

Advanced Research Laboratory, Hitachi Ltd, Kokubunji, Tokyo 185, *Japan*

(*Received* 4 *November* 1987; *accepted* 27 *January* 1988)

Abstract

A new type of *Pendellösung* fringe has been observed which is induced by X-ray resonant scattering very near the absorption edge. Integrated intensities of the 600 reflection from GaAs(100) across the Ga *K* absorption edge, at which X-ray resonant scattering is expected to be significant, were measured. The integrated intensities showed modulations which were caused by the change of the extinction distance due to X-ray resonant scattering or to the change of anomalous scattering factor.

Introduction

With the development of energy-dispersive diffractometry with a solid-state detector combined with continuous radiation from a conventional X-ray anode, integrated reflection intensities from a crystal have been studied very near the absorption edge of the constituent atom of the crystal. X-ray resonant scattering becomes large near the absorption edge, which causes several characteristic features in the diffracted intensities (Fukamachi, Hosoya, Kawamura & Okunuki, 1977, 1979). By using the characteristic changes of intensities, the temperature factors have been determined for a mosaic CuI crystal (Morlon, Fukamachi & Hosoya, 1979, 1981) and for perfect crystals such as GaAs, InSb and Ge (Kawamura & Fukamachi, 1979; Fukamachi, Kawamura, Hayakawa, Nakano & Koh, 1982; Yoshizawa, Kawamura, Fukamachi & Hayakawa, 1986).

The characteristic intensity variations are also applied to determination of anomalous scattering factors $f'(\omega)$ and $f''(\omega)$ (Fukamachi *et al.*, 1977, 1979; Fukamachi & Hosoya, 1975), where $f'(\omega)$ is the real part of the anomalous scattering factor, $f''(\omega)$ its imaginary part and ω the X-ray energy.

Pendellösung fringes are caused by the interference between the incident and diffracted X-rays in a perfect crystal. The fringes were first observed for a wedge-shaped crystal by Kato & Lang (1959). The precise measurement of the period of *Pendellösung* fringes is used to determine the electron density in the crystal (*e.g.* Saka & Kato, 1986) and to determine the anomalous scattering factors (Saka & Kato, 1987). Interference fringes have also been observed as a function of wavelength of the incident X-rays. The period of fringes observed in energy-dispersive integrated reflection intensity is used to determine the electron density and the anomalous scattering factors (Takama, Iwasaki & Sato, 1980).

In this paper, we report the observation of a new type of *Pendellösung* fringe which is induced by X-ray resonant scattering. A large change of $f'(\omega)$ just below the absorption edge of the constituent atom in a crystal causes a change of integrated reflection intensity, which is attributed to *Pendellösung* fringes. We measured the 600 reflection of GaAs across the Ga *K* absorption edge by using an energy-dispersive diffractometer. We used several samples of slightly different thickness to confirm the above interpretation.

Experiment

The samples were GaAs(100) single crystals which contained about 0·04 In atoms in a unit cell. The crystal perfection of the In-doped GaAs was much better than that of the undoped GaAs crystal and the crystal was almost free from lattice defects (McGuigan, Thomas, Barrett, Eldridge, Messham & Swanson, 1986). The dislocation area density of the sample was estimated to be less than 500 cm^{-2} from etch pit distribution (EPD) measurements. The value was much less than the value of 3×10^4 cm^{-2} for the undoped GaAs crystal from EPD measurements. In the following we denote the In-doped GaAs crystal as Ga(In)As. Since the purpose of the present experiment is to detect the *Pendellösung* fringes characteristic of a perfect crystal, it is necessary to use a crystal

0108-7673/88/040433-04$03.00 © 1988 International Union of Crystallography

of high perfection. We will neglect the effect of dopant in the following analysis, although the effect is not necessarily negligible in quantitative analysis.

The experimental setup was the same one as used in a previous study (Yoshizawa *et al.*, 1986). The distance between the anode and the sample was 500 mm and the distance between the sample and the solid-state detector was 220 mm. The effective size of the anode, which was evaluated by considering the size of the anode and the take-off angle, was 0·1 × 10 mm. The slit, 0·2 mm in width, was placed 300 mm from the anode. This slit determined the energy resolution of the reflecting X-rays. To improve the signal-to-noise ratio, the receiving slit, 0·15 mm in width, was set in front of the detector. Diffracted intensities in the Laue case were measured.

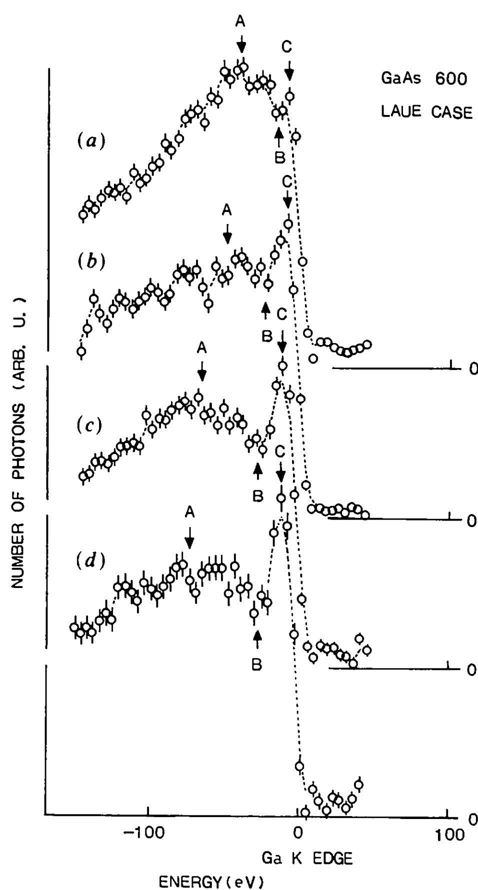

Fig. 1. Measured 600 reflection intensities for a Ga(In)As crystal in the Laue case across the Ga *K* absorption edge. The thickness of the sample is (*a*) 111, (*b*) 127, (*c*) 131 and (*d*) 133 μm. The arrows *A* and *C* indicate the intensity peaks and *B* the dips. In (*a*), the maximum peak counts is 1186 photons in 700 s measurement time. The X-ray generator is operated at 40 kV and 100 mA. In (*b*), the intensity is 1122 counts. The measurement conditions are the same as for (*a*). In (*c*), the intensity is 1178 counts. The measurement time is 1100 s. In (*d*), the intensity is 767 counts. The measurement time is 700 s when operated at 40 kV and 100 mA and 400 s when operated at 40 kV and 150 mA.

Fig. 1 shows the integrated intensities of the 600 reflection from Ga(In)As as a function of X-ray energy. The measured energy ranges from 150 eV below the Ga *K* absorption edge (10 368 eV) to 50 eV above it. The energy step was about 4·4 eV and the energy resolution was 8·4 eV. In general the 600 diffracted intensities are weak and the statistical errors are large. We therefore accumulated enough data to show the oscillatory behavior of intensity. Figs. 1(*a*)–(*d*) correspond to intensity curves for sample thickness of 111, 127, 131 and 133 μm, respectively. In Fig. 1(*a*), a peak is observed, denoted by *A*, around 39 eV below the edge. As the X-ray energy increases, the reflecting intensity decreases and shows a minimum around 14 eV below the edge, denoted by *B*. A weak peak or shoulder appears around 8 eV below the edge (*C*). The intensity drops sharply just below the absorption edge as the X-ray energy is increased. The energy difference between these two peak positions, *A* and *C*, is about 31 eV. In Fig. 1(*b*), the low-energy peak (*A*) shifts to the low-energy side. A peak on the high-energy side (*C*) is more clearly observed and its position is almost the same as in Fig. 1(*a*). The energy difference between these two peak positions is about 40 eV. In Fig. 1(*c*), the two peaks separate more and the energy difference is about 48 eV. The separation of the peak positions becomes about 50 eV in Fig. 1(*d*). The variations of the two peak positions depend on the thickness of the sample, which is reminiscent of *Pendellösung* fringes.

Calculation

By using a dynamical theory of X-ray diffraction with absorption effects taken into account, we calculated the integrated reflection intensities in an energy-dispersive mode. The temperature factor was determined in the same way as described by Yoshizawa *et al.* (1986). We measured the 400 reflection intensities across the Ga *K* absorption edge of Ga(In)As and determined the temperature factor $B = 0{\cdot}83\,(5)$ Å^2 by comparing the intensity ratio below the absorption edge to that above it. Anomalous scattering factors were calculated by use of the formula of Parratt & Hempstead (1954) with the oscillator strengths of Cromer (1965) for *K*, *L* and *M* electrons. The anomalous scattering factors $f'(\omega)$ and $f''(\omega)$ for Ga atoms thus determined are shown in Fig. 2 as a function of X-ray energy. The energy-dispersive integrated reflection intensity was calculated by numerically integrating the intensities for a perfect GaAs crystal neglecting the effect of In dopant. Then we convoluted the intensity with a Gaussian function of the energy width which was determined by the energy resolution of the present optical set up.

The convoluted integrated reflection intensities are shown in Figs. 3(*a*)–(*d*), corresponding to those of

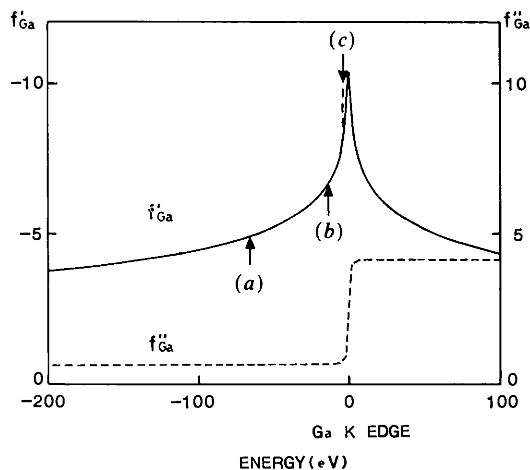

Fig. 2. The anomalous scattering factors $f'_{Ga}(\omega)$ and $f''_{Ga}(\omega)$ near the Ga K absorption edge. The solid line is the real part of the anomalous scattering factor $f'_{Ga}(\omega)$ and the broken line is the imaginary part $f''_{Ga}(\omega)$. The arrows (a), (b) and (c) indicate the energy positions at which the wave field is formed, as shown in Figs. 4 (a), (b) and (c), respectively.

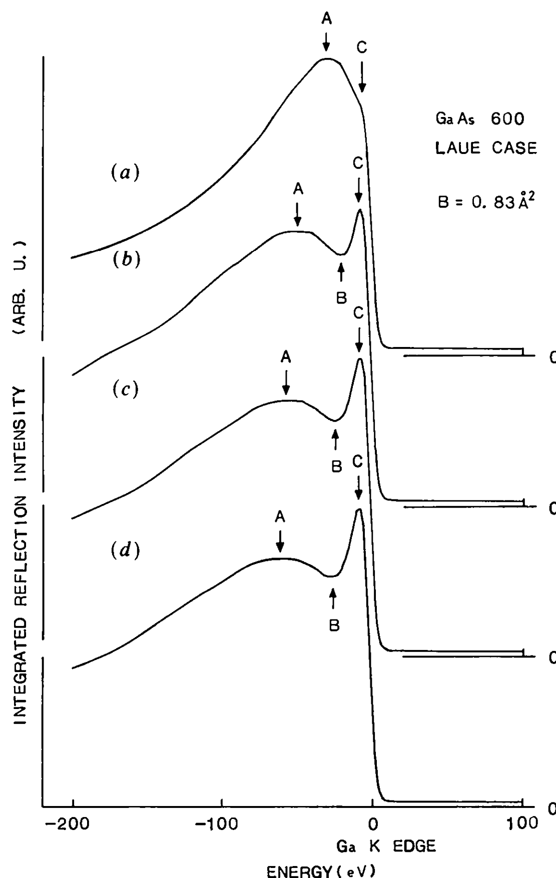

Fig. 3. Calculated values of the 600 integrated reflection intensities in an energy-dispersive mode from a GaAs perfect crystal. The thickness of the crystal is (a) 111, (b) 127, (c) 131 and (d) 133 μm.

Fig. 1. The peak in the low-energy side (A) moves systematically as a function of sample thickness. The peak A appears at 30, 50, 56 and 62 eV below the edge in the respective cases. The peak position in the high-energy side (C) does not move but the peak height shows a systematic variation. The energy difference between the two peak positions becomes large as the sample thickness is increased.

Discussion

If one compares the intensity curves of Fig. 1 with those of Fig. 3, it is noticed that the theory agrees fairly well with the experiment. The position of peak A moves towards the low-energy side as the sample thickness is increased. The width of peak A is relatively large compared with the width of peak C. Peak C appears just below the absorption edge. The peak position does not change, while the height changes as a function of the sample thickness.

The origin of peaks A and C and the dip B is explained as follows. In the X-ray energy range between the absorption edge and 200 eV below it, the real part of the anomalous scattering factor $f'(\omega)$ of Ga ranges from $-10{\cdot}3$ to $-3{\cdot}7$, as shown in Fig. 2. Then the extinction distance of the X-rays varies as a function of energy, which results in a variation of the beating effect between the incident and the diffracted beams in a crystal. The behavior of the beating wave field for the perpendicular components of X-rays is illustrated in Fig. 4. The crystal thickness is assumed to be 133 μm, which corresponds to Fig. 3(d). In the case of Fig. 4(a), the X-ray energy is 66 eV below the Ga K absorption edge and $f'_{Ga} = -4{\cdot}90$. The antinodal plane of the diffracted beam I_h almost coincides with the exit surface, which results in peak A of Fig. 3(d). In Fig. 4(b), the X-ray energy

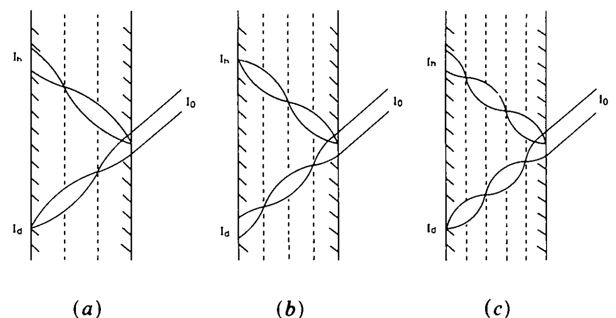

Fig. 4. Schematic illustration of the wave fields inside a crystal when perpendicularly polarized X-rays satisfy the diffraction condition of the 600 reflection for a GaAs crystal in the Laue case. Sample thickness is 133 μm, which is the thickness of the specimen in Fig. 1(d) and Fig. 3(d). I_0 indicates the intensity of the incident beam, I_h that of the diffracted beam and I_d that of the transmitted beam. (a) $f'_{Ga}(\omega) = -4{\cdot}90$, ($b$) $f'_{Ga}(\omega) = -6{\cdot}53$, ($c$) $f'_{Ga}(\omega) = -8{\cdot}00$.

is 15 eV below the absorption edge and the nodal plane of I_h coincides with the exit surface, which gives rise to the dip B of Fig. 3(d). In Fig. 4(c), the X-ray energy is 4 eV below the absorption edge and the antinodal plane of I_h coincides with the exit surface again, which corresponds to peak C. The number of nodes in I_h is two in this case. The intensity variations observed in Fig. 1 are thus attributed to the *Pendellösung* fringes induced by the variation of the real part of the anomalous scattering factor or the X-ray resonant scattering. For the parallel component of the X-rays, the extinction distance is about five times larger than that of the perpendicular component. Less than half a period of the fringe appears for this component and the intensity ratio of a perpendicular to a parallel component is about 5:1. The contribution of the parallel component to the above *Pendellösung* fringe is negligible.

There still remain some discrepancies between theory and experiment. The positions of peak A in Figs. 1(a)–(d) are slightly different from those in Figs. 3(a)–(d). The energy differences between peaks A and C are also different.

In the experiment, the X-ray diffracted intensity was weak for the 600 reflection and the statistical errors were still large for quantitative studies. If we use synchrotron radiation as the incident beam, the diffracted intensity is much higher and the quality of data should be better. The inhomogeneity of the sample thickness is another cause of disagreement between theory and experiment. In the calculation, on the other hand, the most unreliable quantity is the anomalous scattering factor $f'(\omega)$, which affects the intensity curves in Fig. 3 very much. We used the anomalous scattering factor for each isolated atom, which will be slightly different from the corresponding values in the crystal. It has been reported that the real part of the anomalous scattering factor shows some fine structure near the absorption edge (Fukamachi & Hosoya, 1975; Fukamachi *et al.*, 1977, 1979), which is different from $f'(\omega)$ shown in Fig. 2. Another problem in the calculation is that we do not take any dopant (In) effect into account. This will also change the intensity curves but not by so much, because the content of the dopant is only 0·04 atom in a unit cell.

Finally it is noted that we can determine the anomalous scattering factors $f'(\omega)$ very near the absorption edge by comparing theoretical intensity curves with experimental ones as an application of the present study, although experimental elaboration is needed.

The authors express their sincere thanks to Mr Nagasawa of Iwaki Handoutai Corporation for supplying the Ga(In)As sample, and to Professor Nakajima (KEK), Mr Sugawara and Mr Ohshima for their assistance in the experiment.

References

CROMER, D. T. (1965). *Acta Cryst.* **18**, 17–23.
FUKAMACHI, T. & HOSOYA, S. (1975). *Acta Cryst.* A**31**, 215–220.
FUKAMACHI, T., HOSOYA, S., KAWAMURA, T. & OKUNUKI, M. (1977). *Acta Cryst.* A**33**, 54–58.
FUKAMACHI, T., HOSOYA, S., KAWAMURA, T. & OKUNUKI, M. (1979). *Acta Cryst.* A**35**, 828–831.
FUKAMACHI, T., KAWAMURA, T., HAYAKAWA, K., NAKANO, Y. & KOH, F. (1982). *Acta Cryst.* A**38**, 810–813.
KATO, N. & LANG, A. R. (1959). *Acta Cryst.* **12**, 787–794.
KAWAMURA, T. & FUKAMACHI, T. (1979). *Acta Cryst.* A**35**, 831–835.
MCGUIGAN, S., THOMAS, R. N., BARRETT, D. L., ELDRIDGE, G. W., MESSHAM, R. L. & SWANSON B. W. (1986). *J. Cryst. Growth*, **76**, 217–232.
MORLON, B., FUKAMACHI, T. & HOSOYA, S. (1979). *Acta Cryst.* A**35**, 714–717.
MORLON, B., FUKAMACHI, T. & HOSOYA, S. (1981). *Acta Cryst.* A**37**, 92–96.
PARRATT, L. G. & HEMPSTEAD, C. F. (1954). *Phys. Rev.* **94**, 1593–1600.
SAKA, T. & KATO, N. (1986). *Acta Cryst.* A**42**, 469–478.
SAKA, T. & KATO, N. (1987). *Acta Cryst.* A**43**, 252–254.
TAKAMA, T., IWASAKI, M. & SATO, S. (1980). *Acta Cryst.* A**36**, 1025–1030.
YOSHIZAWA, M., KAWAMURA, T., FUKAMACHI, T. & HAYAKAWA, K. (1986). *Acta Cryst.* A**42**, 113–116.